Efficient Photooxygenation Process of Biosourced α-Terpinene by Combining Controlled LED-Driven Flow Photochemistry and Rose Bengal-Anchored Polymer Colloids

Robbie Radjagobalou, Jean-François Blanco, Luca Petrizza, Mickael Le Béchec, Odile Dechy-Cabaret, Sylvie Lacombe-Lhoste, Maud Save, Karine Loubiere

EFFICIENT PHOTOOXYGENATION PROCESS OF BIO-SOURCED α-TERPINENE BY COMBINING CONTROLLED LED-DRIVEN FLOW PHOTOCHEMISTRY AND ROSE BENGAL-ANCHORED POLYMER COLLOIDS

Robbie RADJAGOBALOU[§], Jean-François BLANCO[§], Luca PETRIZZA[‡+], Mickael LE BECHEC[‡], Odile DECHY-CABARET[†], Sylvie LACOMBE[‡], Maud SAVE[‡], Karine LOUBIERE*[§]

[§] Laboratoire de Génie Chimique (LGC), Université de Toulouse, CNRS, INPT, UPS, 4 allée Emile Monso, CS 84234, 31 432 Toulouse, France.

[‡] CNRS, University Pau & Pays Adour, E2S UPPA, Institut des Sciences Analytiques et de Physico-Chimie pour l'Environnement et les Matériaux, IPREM, UMR5254, 64000, Pau.

[†] Laboratoire de Chimie de Coordination (LCC), CNRS, 4 allée Emile Monso, CS 84234, 31 432 Toulouse, France

Corresponding Author

* Karine LOUBIERE. Email : karine.loubiere@toulouse-inp.fr. Phone : (+33) 5 34 32 36 19

ABSTRACT

This work studies the reactivity of poly(*N*-vinylcaprolactam-co-vinyl acetate-co-vinylbenzyl Rose Bengal) microgels (VBRB@MG) as heterogeneous photosensitizers in a continuous-flow process for sustainable singlet oxygen sensitized photooxygenation of a bio-based molecule. Experiments were carried out in a LED-driven spiral-shaped microreactor in which slurry Taylor flows were generated, allowing accurate control of irradiation, light absorption and gas-liquid flow conditions. The benchmark photooxygenation of α-terpinene was implemented in ethanol to provide a green solvent using air as a safe supply of oxygen. Swollen RB-grafted colloids formed an efficient substrate for converting α-terpinene into ascaridole, providing up to high conversion with high selectivity under continuous-flow conditions, and within short residence times of a few minutes. The supported RB exhibited a reactivity similar to that of the free RB. The reactivity of the supported photosensitizer was maintained for several cycles with a reproducible level after 8 months of storage. Under experimental conditions favouring photobleaching of RB, the photobleaching level of RB was lower with the VBRB@MG colloids than with free RB, suggesting that grafting RB molecules onto the colloid can prevent their photodegradation.

KEYWORDS

Flow photochemistry. Singlet oxygen. Photoactive polymer colloids. Green conditions. Rose Bengal. Alpha-terpinene.

INTRODUCTION.

Organic photochemistry is a key synthetic pathway for sustainable chemistry. [1,2,3] Multi-step syntheses of complex molecules are shortened and simplified, a portfolio of novel chemicals becomes accessible, and the photon acts as a "traceless reagent". **Erreur ! Source du renvoi introuvable.**4-7 Several fundamental principles of Green Chemistry are thus addressed by photochemistry.[8] Among the photochemical processes, photooxygenation reactions are very attractive as they involve only singlet oxygen ($^1O_2$), a powerful selective oxidant, which is produced by safe photosensitization of oxygen in the visible range and at ambient temperature.[9] Singlet oxygen photosensitization corresponds to an energy transfer from catalytic amounts of an organic dye (photosensitizer) to molecular ground-state oxygen (triplet).[10] Photooxygenation reactions have proved to be very efficient for the preparation of endoperoxides from biosourced molecules such as terpene and furanone derivatives.[11-13] Only a limited number of these transformations can be carried out thermally, as they require the use of complex oxidants containing either hazardous peroxides or hypervalent iodine compounds or metal catalysts. Thus, from an atom economy point of view, photooxygenations are of interest as their only requirements are catalytic amounts of a metal-free organic photosensitizer and molecular oxygen as an oxidant. It is also noteworthy that sensitized photooxygenations find applications not only in the synthesis of fine chemicals, [14] but also in wastewater treatment or in the degradation of insecticides and pesticides.[15-17]

The implementation of organic photooxygenations at industrial scale are limited to a few examples in the flavour, fragrance or pharmaceutical industries.[18-21] Batch reactors equipped with energy-demanding light sources are the main systems currently used for industrial photooxygenation set-ups. Non-eco-friendly solvents are generally used to maximize the singlet oxygen lifetime, and the photosensitizer (as solid powder) is regularly fed to minimize its

degradation. Continuous-flow microstructured technologies, which involve channels or tubes from tens of micrometres to a few millimetres in diameter are now recognized as alternatives to batch processing. Their benefits for organic photochemistry have been highlighted recently.[22-28]**Erreur ! Source du renvoi introuvable.** The integration of LEDs (Light-Emitting Diodes) as light sources in these technologies provides new opportunities. They present high electrical yields, long lifetimes, and spatial compactness, with the possibility of selecting the emission spectral domain and modulating the emitted radiant power.[29,30]

Most of the literature related to LED-driven flow photochemistry considers a sensitizer solubilized in the reaction medium.[31-36] In parallel, the concept of solid-supported sensitizers offers many advantages as it makes it easier to separate the organic sensitizer from the other reactants and products, avoiding expensive downstream separation.[37-46] It is also a strategy for transposing poorly soluble photosensitizers into green solvents, while simultaneously enhancing their photostability and reusability. Solid-supported sensitizers in continuous-flow microstructured reactors were first implemented in the form of polymer/silica films cast onto the walls of the reactor. [47-49] However, the light that can be delivered per specific surface area of the reactor is significantly reduced in this configuration and the replacement of the substrate film is complex. Including porous monoliths or packed porous beads with finely tuned particle sizes in continuous-flow reactors has been reported as an alternative strategy. [50-56] Although it may be particularly suitable at lab-scale for material screening or reusability tests, transfer towards industrial production remains quite challenging: long reactors with narrow diameters are indispensable to avoid light limitations while reaching sufficient residence times for full conversions without resorting to a multi-pass mode. Such devices are also faced with issues related to high pressure drops and consumption of solvent. Consequently, the most

straightforward suitable method in a perspective of a scale-up is to operate with a suspension of the small particles grafted with the sensitizer, and to transport this suspension by the flow from the inlet to the outlet of the microreactor. As a continuous flow of bubbles (air or pure oxygen) remains the most preferable option to supply oxygen to the reaction medium, this leads to operation under gas-liquid slurry flows (Figure 1). Such a concept has been successfully applied in microreactors for catalytic hydrogenation applications[57-59] but to date, only two studies have been reported for photooxygenation, and involved either conjugated microporous polymers (CMPs)[56] or functionalized mesoporous silica particles.[60] The most relevant strategy for achieving good operability appears to be the implementation of submicronic materials covalently grafted to an efficient organic photosensitizer. Their smaller sizes mean that they are not prone to settle (in particular at the microreactor walls where the velocities are very low), unlike micrometric beads (such as the commercial Sensitox® polystyrene particle). The challenge in the design of the polymer colloid materials as a photoactive heterogeneous substrate is to make an efficient contact possible between the grafted photosensitizer, oxygen, and the molecule to be oxidized. The average diffusion length of $^1O_2$ is only tens of nanometres in a dense polymer,[10] while it is hundreds of nanometres, on average, in alcoholic media (the diffusion length being a combination of $^1O_2$ lifetime in a surrounding medium and its diffusion rate).[61,62]

As ethanol is one of the green solvents of reference for most photooxygenation of bio-based molecules, Rose Bengal photosensitizer-grafted polymer microgels exhibiting swelling ability in ethanol bring together most of the targeted relevant properties.[63] These microgels were synthesized by an eco-friendly solvent-free polymerization process carried out in aqueous dispersed media.[63] Rose Bengal (RB) photosensitizer offers interesting features as it is metal-free, non-toxic, commercially available, cheap, already used at industrial scale, and soluble in

polar-protic solvents. It also exhibits intensive absorption bands in the visible range with a good singlet oxygen quantum yield in ethanol ($\phi_{^1O_{2,ethanol}} = 0.75$).[64,65]

In the present work, the photoreactivity of poly(*N*-vinylcaprolactam-*co*-vinyl acetate-*co*-vinylbenzyl Rose Bengal) microgels (VBRB@MG) as heterogeneous photosensitizers will be investigated in a continuous-flow process for sustainable singlet oxygen sensitized photooxygenation of a bio-based molecule. Their efficiency will be investigated under accurate control of irradiation, light absorption and flow conditions. We will focus on the effects of both oxygen stoichiometry and medium absorbance on the photochemical kinetic law in such gas-liquid slurry flows as it is crucial for further implementation at a larger scale. Here, the photooxygenation of α-terpinene (Scheme 1) is carried out as a benchmark reaction in a dedicated LED-driven continuous microreactor (Figure 1). The performances, in terms of yield of photooxygenation, selectivity and photobleaching, of heterogeneous RB covalently anchored onto microgel are systematically compared to those of free soluble RB. Finally, the reusability of the photoactive colloids is assessed by monitoring the yield of α-terpinene after several photooxygenation cycles.

EXPERIMENTAL SECTION

Photooxygenation reaction. Ascaridole was the main product of the photooxygenation of α-terpinene, with the minor product p-cymene (Scheme 1, top).[33] Isoascaridole could be also formed from ascaridole by thermal isomerization (Scheme 1, bottom).[38] All the experimental details are described in Part S.1 of the Supporting Information.

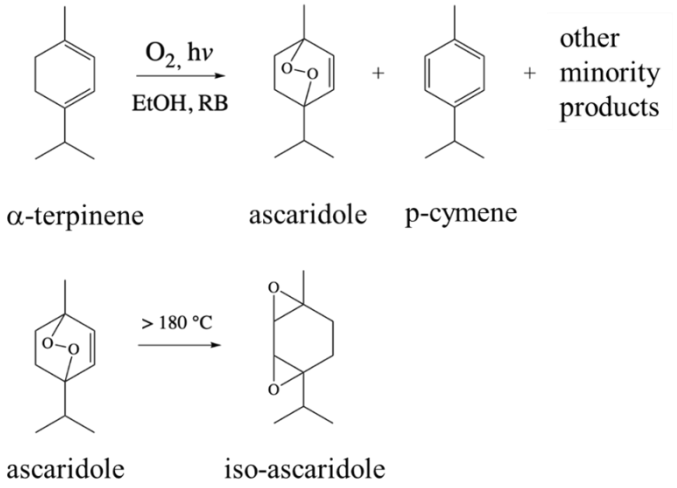

Scheme 1. Photosensitized oxygenation of α-terpinene (top). Thermally induced isomerization of ascaridole to iso-ascaridole (bottom).

Photoactive polymer colloids. Photoactive colloids were synthetized by miniemulsion copolymerization of vinyl acetate (VAc), N-vinyl caprolactam (VCL), divinyl adipate (DVA) crosslinker and vinyl benzyl Rose Bengal (VBRB) monomer as previously reported.[63] The continuous phase was a water phase and the polymerization took place in the monomer droplets created by ultrasonication. Two types of microgels were used in this work (see Table S.1): VBRB@MG-8 and VBRB@MG-14 with respectively 8 mol-% or 14 mol-% of DVA crosslinker based on the overall amount of monomers and crosslinker. For both microgels, 0.70 mol % of VBRB was initially introduced. After their synthesis in water, the microgels were systematically redispersed in ethanol and immediately stored in the fridge at 4 °C. The so-called storage period corresponded to the duration between the synthesis of the microgels and the first use under continuous-flow photooxygenation conditions.

The UV-visible spectra of VBRB@MG-8 and VBRB@MG-14 in ethanol (Figure S.1) showed that the wavelength at which the absorption of grafted RB was maximal, noted λ_{max} (nm), was

569 nm and thus slightly longer than that of free RB in ethanol (λ_{max} = 557 nm), highlighting a bathochromic effect. TEM analysis revealed a quasi-spherical shape of colloids.[63] The main colloidal features of microgel dispersed in water or ethanol are reported in Table S.1, together with values of singlet oxygen quantum yield of VBRB anchored in the microgels dispersed in ethanol and the photosensitizer loading. It should be highlighted that both microgels proved to be photoactive in ethanol phase as the values of singlet oxygen quantum yield, $\phi_{^1O_2}$ (-), defined by the ratio of the number of moles of singlet oxygen produced to the number of moles of photon absorbed by the photosensitizer, ranged from 0.27 – 0.35 (Table S.1).[63] The efficiency in producing singlet oxygen under irradiation was mainly due to their ability to swell in ethanol, thus favouring the diffusion of oxygen and reactive species in the vicinity of the grafted photosensitizer. This is an interesting feature of these microgels. We previously demonstrated that the VBRB@MG microgels dispersed in water were not able to produce singlet oxygen as the polymer was in a collapsed state inside the microgels.[63] Note that the linear P(VCL-*co*-VAc) chains forming the polymer network were soluble in ethanol but insoluble in water.[66] As generally observed for supported photosensitizers, values of $\phi_{^1O_2}$ of VBRB@MG remained lower than that of free Rose Bengal in ethanol ($\phi_{^1O_2}$= 0.75), [65] which could arise from the polymeric confinement of the photosensitizers and/or from structural modifications. However, the present singlet oxygen quantum yields were rather high when compared with other supported RB.[40] The average loadings of VBRB@MG (Table S.1) were estimated at almost 215 ± 30 $\mu mol_{RB}.g_{driedMG}^{-1}$, and thus higher than the value for commercially available Sensitox® micrometric particles (about 100 $\mu mol_{RB}.g_{polymer}^{-1}$).

LED-driven microreactor. The homemade microreactor consisted of an FEP tube fixed in a channel carved in a flat plate aluminium substrate, and wound into an Archimedean spiral, as illustrated in Figure 1.[67,68,69] Thanks to this in-plane spiral-shaped geometry, the device was compact (160 × 160 mm^2), and allowed the irradiation to be perfectly controlled over the whole tubing surface, in terms of both homogeneity and photon flux, while offering the possibility of long residence times.

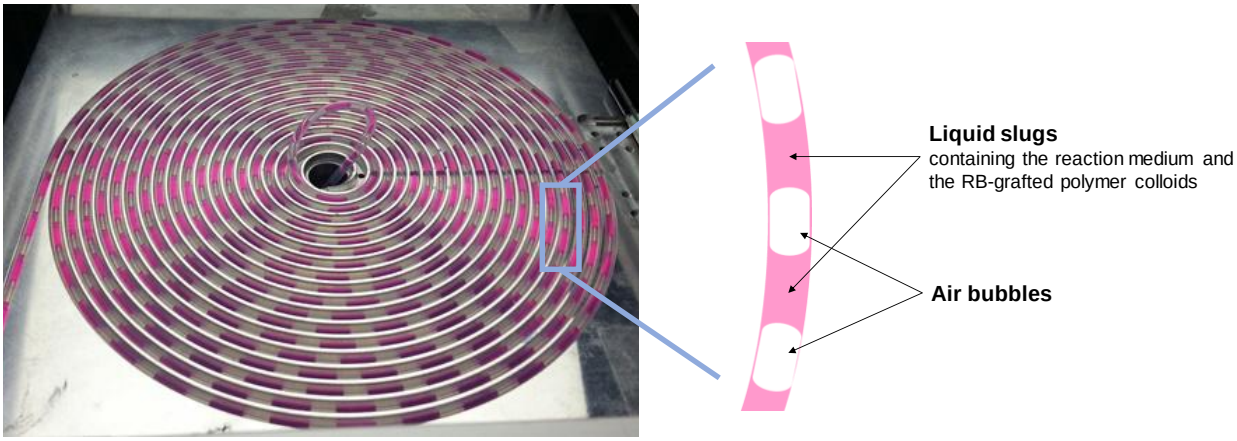

Figure 1. Picture illustrating the Archimedean spiral geometry of the LED-driven microreactor in which the slurry Taylor flow was generated.

The inner and outer diameters of the tubing were respectively 1 mm and 3.2 mm and the length was 5 m (almost 18 spirals). The reactor volume, noted V_R (m^3), was 3.93 mL. The irradiated specific area, a_{irrad} (m^{-1}), defined as the ratio of the irradiated surface of the microreactor to the volume of the reactor, was estimated to be close to 1000 m^{-1} (considering a one-dimensional SLAB geometry and a characteristic optical path length equal to the inner diameter of the FEP tubing, namely 1 mm). The spiral-shaped microreactor was illuminated by a purpose-built visible-LED array manufactured by the company Led Engineering Development (Montauban, France), described in Part S.4 of the Supporting Information and shown in Figure S.2. In the

present study, the photon flux densities measured at the microreactor surface, noted q_r ($\mu mol_{photon}.m^{-2}.s^{-1}$), were equal either to 1440 or to 2134 $\mu mol_{photon}.m^{-2}.s^{-1}$.

All experiments were carried out under Taylor flow conditions, i. e. stable segmented flows of air bubbles regularly spaced between liquid slugs were obtained in the tube (see Part S.5. of the Supporting Information). The spatial distribution of gas and liquid phases inside the tube (i. e. the size of air bubbles and of the liquid slugs) was controlled by the volumetric ratio, noted q, defined by the ratio between the air volumetric flow rate, Q_G, and the liquid volumetric flow rate, Q_L, according to Eq. 1:

$$q = \frac{Q_G}{Q_L} \qquad \text{(Eq. 1)}$$

When the gas and liquid volumetric flow rates were changed, the stoichiometric ratio between oxygen and α-terpinene at the inlet of the microreactor was also modified. It was then possible to define the ratio between the molar flow rates of oxygen (F_{O_2}) that could be delivered by each bubble, and the molar flow rate of α-terpinene ($F_{\alpha T}$), noted f, according to Eq. 2

$$f = \frac{F_{O_2}}{F_{\alpha T}} \qquad \text{(Eq. 2)}$$

The definitions of these flow rates and the relationships between them, the residence time, τ (s), and the initial concentration of α-terpinene, $C_{\alpha T,0}$ ($mol.L^{-1}$), are detailed in Part S.6. of the Supporting Information.

General procedure for the photooxygenation of α-terpinene under continuous flow using VBRB@MG photoactive colloids. For a given set of operating conditions, when steady-state was reached, the samples (of a few mL) were collected in an amber glass at the outlet of the microreactor. They were analysed immediately, thus preventing any evolution of the reaction

medium between collection and analysis. The analytical methods have already been described by Radjagobalou *et al.* [33] The RB-photobleaching level, χ_{RB} (-), was calculated as the ratio of the concentration of the photobleached photosensitizer with respect the initial concentration of RB (see Part S.7 of the Supplementary Information).

The conversion of α-terpinene, $\chi_{\alpha T}$, was defined according the concentration of α-terpinene measured (Gas Chromatography measurements) at the inlet and outlet of the microreactor (see Part S.8 of the Supplementary Information). For all the photooxygenation experiments, it was shown that the conversion of α-terpinene could be considered equal to the yield of ascaridole, as no impurities were detected except the ones initially present in the starting material. A high selectivity was thus obtained.

Experiments were carried out in the spiral-shaped microreactor, using the synthetized photoactive colloids or free RB (i. e. RB directly solubilized in ethanol), for comparison. As far as possible, both types of experiments were compared at similar absorbances of the reaction medium measured at λ_{max}, at the inlet of the microreactor (noted $A_{\lambda_{max},0}$) in order to work under identical light attenuation conditions. Note that, for both cases (free RB or photoactive colloids), the values of the absorbance of the reaction medium inside the microreactor were kept smaller than unity in all the experiments. This thus corresponded to conditions where the characteristic optical path length, $\bar{\delta}$ (m), is smaller than the characteristic light penetration distance, d_{pen} (see Part S.7. of the Supporting Information). Consequently, under these conditions, the medium could not be considered “fully absorbing”: the part of the incident flux not absorbed by the RB molecules (typically 10 - 20 %) was thus transmitted over the back optical wall of the microreactor.

A specific procedure was applied to the synthetized photoactive colloids before their implementation in the microreactor: the solvent was changed (from water to ethanol), and the related suspension was made to flow, without irradiation, in the microreactor for a certain time (see Part S.9. of the Supporting Information).

The initial concentration of α-terpinene, $C_{\alpha T,0}$, was 0.035 mol.L^{-1} or 0.100 mol.L^{-1}. Based on the results obtained by Radjagobalou *et al.*,[33] the ratio between the gas and liquid volumetric flowrates, *q*, was set equal to 5, corresponding to long bubble lengths (~ 1.8 cm) and short liquid slug lengths (~ 0.4 cm). According to the values of $C_{\alpha T,0}$ and *q*, the stoichiometry ratio *f* was equal either to 1.5 (for $C_{\alpha T,0}$ = 0.035 mol.L^{-1}) or to 0.5 (for $C_{\alpha T,0}$ = 0.100 mol.L^{-1}), involving conditions respectively above and below stoichiometry in terms of oxygen compared to α-terpinene . More details about the calculations of these parameters are given in Part S.6 of the Supporting Information.

RESULTS AND DISCUSSION

A first series of photooxygenation of α-terpinene was carried out under continuous flow using VBRB@MG-8 and VBRB@MG-14 microgels as heterogeneous photosensitizers (Figure 2).
For both VBRB@MG microgels, the grafted photosensitizer efficiently produced singlet oxygen, quantitatively converting α-terpinene into ascaridole (conversion above 80 %, selectivity close to 98 %) in a short residence time (< 4 min). Several reasons could be provided to explain these good results. Firstly, this type of technology allows a short light penetration distance (~ 1 mm) while offering a high irradiated specific area (~ 1000 m^2.m^{-3}). The extensive flux of photons per unit of liquid volume (~ 1400 - 2500 $\mu mol_{photon}.m^{-3}.s^{-1}$) makes possible to reduce the irradiation

times significantly in comparison to conventional batch photoreactors (typically varying from ten minutes to several hours)[28], even for concentrated chromophore solutions. In addition, gas-liquid Taylor flow allows very efficient mixing (i. e. frequency of contact) between reactive species as the recirculation times inside the liquid slugs between two consecutive bubbles vary typically between 10 and 100 milliseconds.[68] The gas-liquid Taylor flow also induces an intensification of the mass transfer of oxygen from gas bubbles to the reaction medium: the overall volumetric gas-liquid mass transfer coefficients typically range from 0.1 to 2 s^{-1}, which is tens of times or even a hundred times higher than in batch photoreactors.[69] The high conversions observed would be also the result of the very good external liquid-solid mass transfer coefficients that can be achieved in slurry Taylor flows due to the transport of the suspension by means of internal vortices occurring in the liquid slugs of the segmented flow.[70,71]

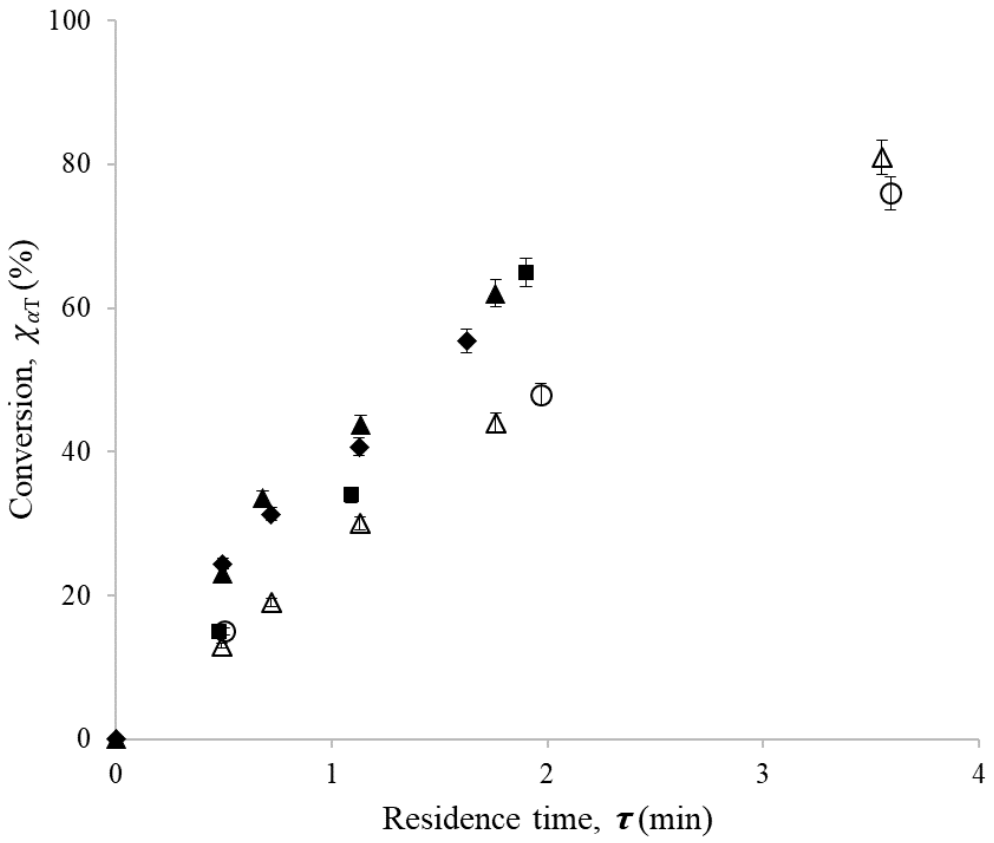

Figure 2. Conversion of α-terpinene, $\chi_{\alpha T}$, versus residence time, τ, for the photoactive colloids after various times of storage. Empty and full symbols correspond to $A_{\lambda_{max,\,0}} = 0.05$ and $A_{\lambda_{max,\,0}} = 0.10$, respectively. Full squares are related to a storage period of 3 months for VBRB@MG-8 (■), full diamonds to a storage period of 6 months for VBRB@MG-14 (♦), full triangles to a storage period of 8 months (▲) for VBRB@MG-14. Empty circles and triangles are related to a storage period of 1 month (○) and 8 months (Δ) for VBRB@MG-14. Conditions: $C_{\alpha T,0}$ = 0.035 mol.L^{-1}, q = 5, f ~ 1.5, q_r = 1440 $\mu mol_{photon}.m^{-2}.s^{-1}$. The concentrations of the photoactive colloids were close to 0.025 g $_{driedMG}.L^{-1}$ and to 0.050 g $_{driedMG}.L^{-1}$ for $A_{\lambda_{max,\,0}} = 0.05$ and for $A_{\lambda_{max,0}} = 0.10$, respectively.

In Figure 2, the photooxygenation kinetics are presented at different storage periods for both photoactive colloids. Over the eight months of storage, the variations of the conversion of α-

terpinene with residence time remained similar for VBRB@MG-14 colloids. They also almost overlapped with the one of VBRB@MG-8 after 3 months of storage, despite the slight difference in singlet oxygen quantum yields ($\phi_{^1O_2}$= 0.27 for VBRB@MG-8 and $\phi_{^1O_2}$= 0.35 for VBRB@MG-14, Table S.1). Moreover, longer residence times were required to achieve high conversions when the absorbance of the reaction medium was decreased (i. e. when the concentration of the photoactive colloids decreased). For instance, for VBRB@MG-14 after a storage period of 8 months, 62 % and 44 % of conversion were achieved at a residence time of 1.76 min for $A_{\lambda_{max,0}}$= 0.1 and $A_{\lambda_{max,0}}$= 0.05, respectively. Such a trend is in agreement with the results observed using free RB.[33] It is interesting to note that, for all the experiments reported in Figure 2, no photobleaching of the RB grafted onto the microgels was observed (see Part S.10 of the Supporting Information).

In conclusion of this part, it can be noted, first, that the slight differences of hydrodynamic diameters and singlet oxygen quantum yields (see Table S.1) between the two solid photosensitizer substrates (VBRB@MG-8 and VBRB@MG-14) had no influence on the kinetics of α-terpinene conversion under the operating conditions tested. Second, their reactivity was stable over 8 months of storage with good reproducibility. After the synthesis, the colloids could thus be stored for 8 months and used without any change of properties and/or photooxygenation performances, an interesting criterion not often scrutinized in the literature.

The following series of experiments was intended to demonstrate the ~~efficiency~~ potentiality of flow photochemistry combined with photoactive colloids. For this purpose, the photooxygenation of α-terpinene was deliberately investigated under less favourable conditions. Ethanol was again chosen as a green solvent even though the lifetime of singlet oxygen is known

to be shorter in ethanol than in less eco-friendly chlorinated solvents (13.5 μs in ethanol versus 160-265 μs in chlorinated solvents).[72] To implement a safe and easy process, the oxygen was obtained from the air instead of using a source of pure oxygen. The selected Rose Bengal photosensitizer has a strong ability to degrade by photobleaching, which could be explained by structural alterations under UV light exposure and/or a secondary electron transfer reaction when α-terpinene reacts with an excited Rose Bengal molecule to form p-cymene and a reduced form of Rose Bengal.[73,74]

Figure 3 compares the photooxygenation rates between the RB-grafted polymer colloids dispersed in ethanol and the free RB photosensitizer in ethanol. This comparison was made for different initial concentrations of RB photosensitizer, characterized by different values of absorbance, $A_{\lambda_{max,\,0}}$, ranging from 0.05 to 0.5, at the inlet of the microreactor. The configuration was set with a molar excess of oxygen compared to α-terpinene (f ~ 1.5, see Eq. 2 and Part S.6. of the Supporting Information).

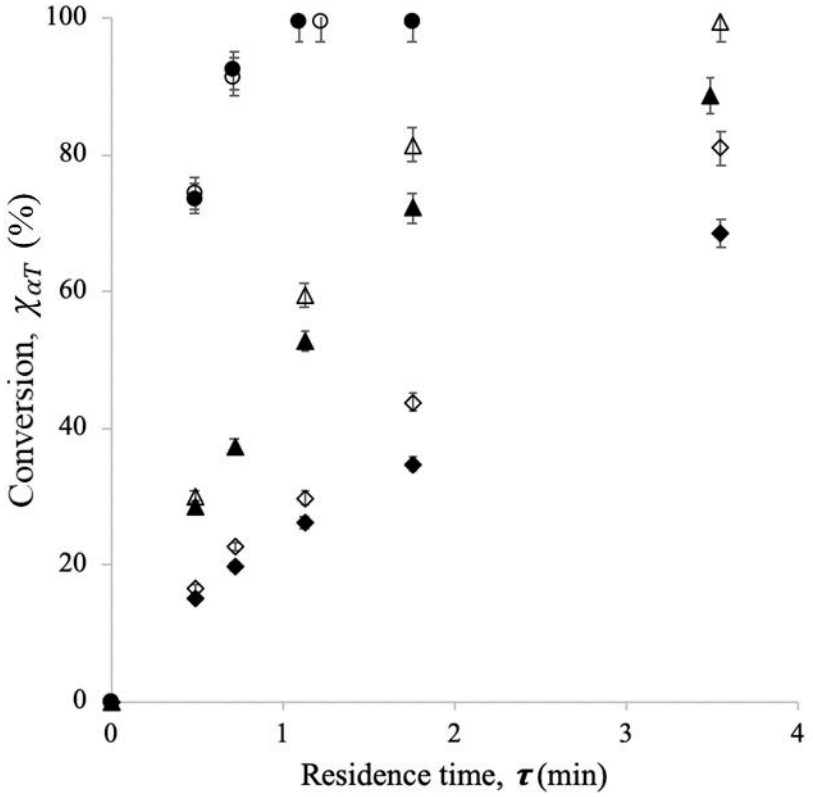

Figure 3. Conversion of α-terpinene, $\chi_{\alpha T}$, versus residence time, τ. Empty symbols correspond to VBRB@MG microgels and full symbols to free Rose Bengal. For different values of absorbance measured at λ_{max} at the inlet of the microreactor: $A_{\lambda_{max},0}$=0.500 (● free RB, ○ VBRB@MG-8), $A_{\lambda_{max},0}$=0.130 (▲ free RB), $A_{\lambda_{max},0}$=0.135 (Δ VBRB@MG-8), $A_{\lambda_{max},0}$=0.065 (♦ free RB), $A_{\lambda_{max},0}$=0.050 (◊ VBRB@MG-14). Operating conditions: $C_{\alpha T,0}$ = 0.035 mol.L^{-1}, q = 5, q_r = 1440 $\mu mol_{photon}.m^{-2}.s^{-1}$, f ~ 1.5.

First, it is interesting to note that the photobleaching level of RB, χ_{RB} , remained below a few percent for the experiments carried out with free Rose Bengal (see Part S.10 of the Supporting Information). This result is in agreement with our previous results,[33] demonstrating that an excessive amount of oxygen compared to α-terpinene minimized the RB photobleaching.

Interestingly, the same trend was observed for the experiments with photoactive colloids (see Part S.10 of the Supporting Information).

Figure 3 shows that, for a given absorbance, the supported RB exhibited a reactivity similar to that of the free RB. High conversions of α-terpinene (Figure 3) with a high selectivity in ascaridole (Figure S.7) were achieved in a few minutes of residence time. Increasing the initial grafted RB concentration (i. e. a higher initial absorbance) led to faster kinetics as for free RB. For instance, with supported RB, for $A_{\lambda_{max,0}} = 0.05$, a residence time of 1.13 min led to a conversion of 30 %, while for $A_{\lambda_{max,0}} = 0.5$, a conversion of 99 % was obtained with the same residence time.

The ability of VBRB@MG to produce singlet oxygen clearly demonstrates the relevance of implementing submicronic colloidal photoactive microgels, able to swell in ethanol, as supported photosensitizer in a LED-driven microreactor. As the singlet oxygen quantum yield ($\phi_{^1O_2}$) measured in batch was twice as high for free RB as for supported RB (see Table S.1), [63] the very close correlation between the variation of the conversion of α-terpinene and the residence time observed between photoactive colloids and free RB (Figure 3) suggests that more complex physicochemical and photophysical phenomena occur in the vicinity of and/or inside the colloids. For instance, the local concentration of the various species including singlet oxygen, substrate and product, inside the swollen microgels or the lifetime of singlet oxygen could be different in the heterogeneous medium and in ethanol. Also, the presence of photoactive colloids could change the gas-liquid flow properties as these types of colloids are known for their propensity to adsorb at the bubble surface.[75,76,77] This could induce some modifications in terms of gas-liquid hydrodynamics, such as bubble velocity and size, thickness of the liquid lubrication film at the walls, or liquid velocity field in the liquid slug. The interfacial gas-liquid mass

transfer, and thus the amount of oxygen transferred from the bubbles per unit of time, could be modified in return. In the latter case, the fact that the observed variations of conversion with residence time are the same between colloids and free RB might reveal some more favourable operating conditions. Deeper investigations will be required to clarify these questions and thus to better understand these promising results.

The third series of experiments aimed at evaluating the resistance of the grafted-RB molecules to photobleaching, in particular in comparison with free RB. For this purpose, the operating conditions were modified. First, a stoichiometric excess of α-terpinene compared to oxygen was used at the inlet of the microreactor, in order to increase the probability of reaction between α-terpinene and excited RB, giving rise to both p-cymene and photobleached RB. This is a way to better highlight a difference in RB photobleaching between the free photosensitizer and the supported one.[33] In consequence, in the series of experiments reported in Figure 4, an initial α-terpinene concentration of 0.105 $mol.L^{-1}$ (instead of 0.035 $mol.L^{-1}$) was imposed, leading to a stoichiometric ratio f equal to 0.5 (instead of 1.5). The photon flux density at the microreactor surface was also increased from 1440 to 2184 $\mu mol_{photon}.m^{-2}.s^{-1}$, in order to increase the amount of photo-excited species produced per unit of time. The photooxygenation reaction was implemented at two different initial concentrations of photosensitizer by setting the initial absorbance of the medium at either 0.15 or 0.70.

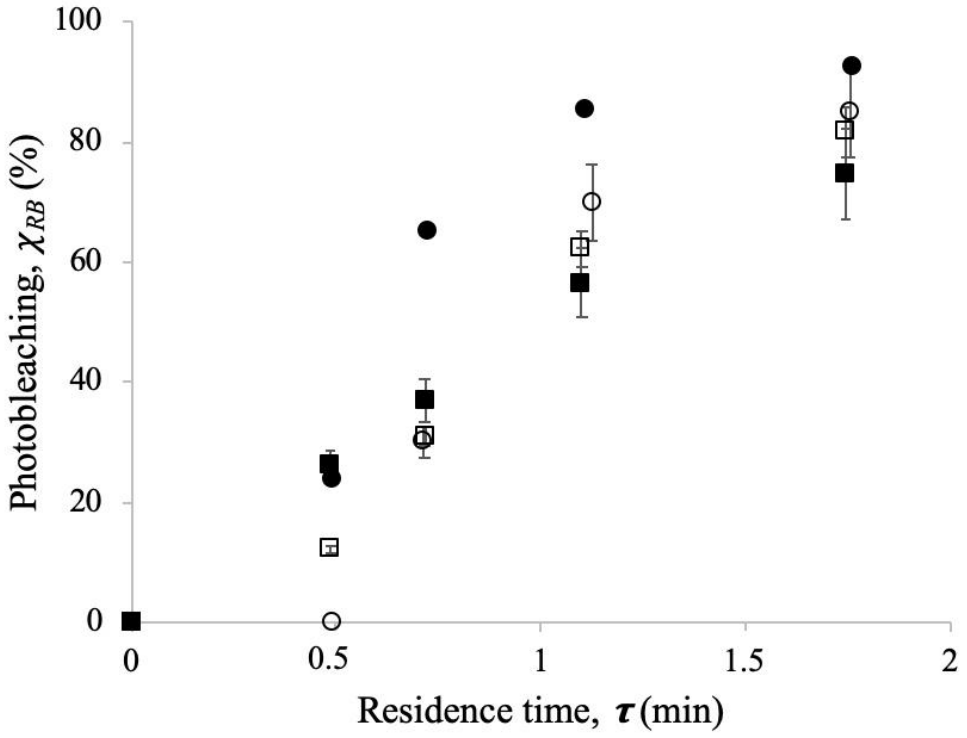

Figure 4. Photobleaching level of RB, χ_{RB}, versus residence time τ for different values of absorbance at the inlet of the microreactor: $A_{\lambda_{max,0}}$=0.70 (● free RB, ○ VBRB@MG-14), $A_{\lambda_{max,0}}$=0.14 (■ free RB), $A_{\lambda_{max,0}}$=0.16 (□ VBRB@MG-8). Operating conditions: $C_{\alpha T,0}$ = 0.105 mol.L^{-1}, q = 5, q_r = 2184 µmol$_{photon}$.m^{-2}.s^{-1}, f ~ 0.5. Empty symbols correspond to VBRB@MG microgels and full symbols to free Rose Bengal.

Figure 4 displays the evolution of the photobleaching levels of RB with the residence times for RB-grafted colloids and free RB. Note that, because the experiments were carried out with a stoichiometric excess of α-terpinene, the conversion of α-terpinene was incomplete (< 50 %) and reached a plateau (see Figure S.9) while the photobleaching level reached 75 % to 90 % at 1.7 minutes of residence time. For the smallest concentration of RB photosensitizer ($A_{\lambda_{max,0}}$ = 0.15), no major difference was observed between grafted and free RB. Interestingly, for the highest concentration of RB photosensitizer ($A_{\lambda_{max,0}}$=0.70), the VBRB@MG colloids

allowed a decrease of 24 % in the photobleaching level between 0.5 and 1 min, and a decrease of 10 % between 1 and 2 min, compared to free RB. Thus, for a strong absorbing medium, the covalent anchoring of RB molecules inside submicronic polymer colloids could prevent their photodegradation. This finding is in agreement with the observations made by Petrizza *et al.*[63] and is particularly interesting since the "optimal conditions" for operating a photoreactor correspond to an absorbance of photosensitizer close to one. [28]**Erreur ! Source du renvoi introuvable.**

The objective of the last series of experiments was to evaluate the possibility of reusing the photoactive colloids for several photooxygenation cycles. Based on the previous results, two sets of experimental conditions ($C_{\alpha T,0}$; q_r) were considered to cover two types of operating domains:

- Case 1: ($C_{\alpha T,0}$ = 0.035 mol.L^{-1}; q_r = 1440 µmol$_{photon}$.m^{-2}.s^{-1}), preventing RB photobleaching.
- Case 2: ($C_{\alpha T,0}$ = 0.100 mol.L^{-1} of α-terpinene; q_r = 2184 µmol$_{photon}$.m^{-2}.s^{-1}), favourable to RB photobleaching.

The procedure used is described in Part S.11 of the Supporting Information.

Figure 5 reports the conversion of α-terpinene, $\chi_{\alpha T}$, and the photobleaching level of RB, χ_{RB}, after each cycle, *i*, of photooxygenation in the LED-driven spiral-shaped microreactor (all the related numerical values are reported in Part S.11 of the Supporting Information). For Case 1 (stoichiometric excess of oxygen), whatever the number of cycles (from 1 to 4), the α-terpinene conversions were almost identical (~ 33%) and no photobleaching occurred (~ 0.11 %). This is a key point showing that the photoactive colloids can be reused for several cycles. As expected, Case 2 (stoichiometric excess of α-terpinene) led to significantly higher photobleaching levels (~

27 %) than Case 1 (~ 0.11%) for each cycle. Due to the photosensitizer photodegradation, lower conversions were observed, with a slight decrease from cycle 1 to cycle 4 (from 21 to 13 %).

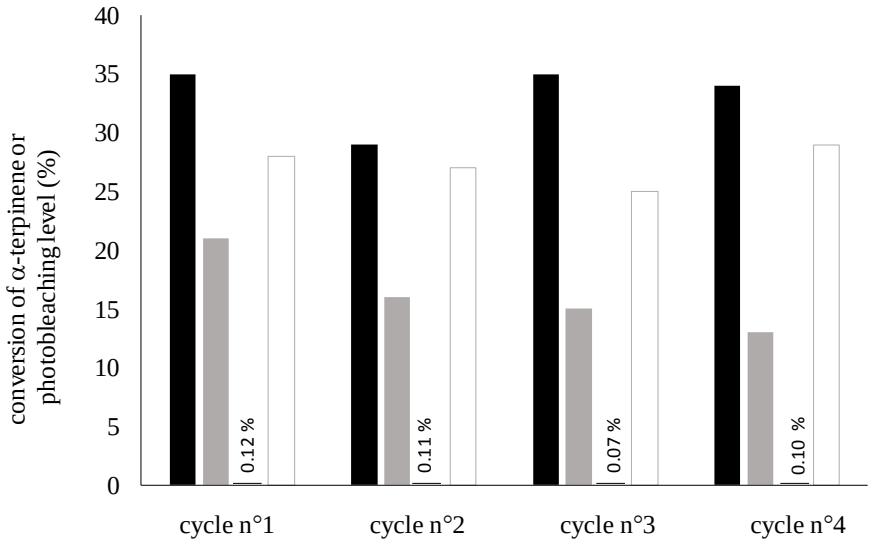

Figure 5. Conversion of α-terpinene (full bars) and photobleaching level of RB (empty bars) after each cycle, *i*, of photooxygenation in the LED-driven spiral-shaped microreactor. Black bars correspond to Case 1, and grey bars to Case 2. Operating conditions for Case 1: VBRB@MG-8; A_{569} = 1.46; $C_{\alpha T,0}$ = 0.035 mol.L^{-1};; f = 1.6; τ = 0.5 min; q_r = 1440 µmol$_{photon}$.m^{-2}.s^{-1}. Operating conditions for Case 2: VBRB@MG-14; $C_{\alpha T,0}$ = 0.100 mol.L^{-1}; A_{569} = 1.80; f = 0.5; τ = 0.72 min; q_r = 2184 µmol$_{photon}$.m^{-2}.s^{-1}. Note that, for Case 1, as the related photobleaching level was too small, the related values are directly indicated in the figure and no corresponding black empty bar is plotted.

CONCLUSION

This study has shown the photoreactivity efficiency of poly(N-vinylcaprolactam-co-vinyl acetate-co-vinylbenzyl Rose Bengal) microgels as heterogeneous photosensitizers in a continuous-flow process for sustainable singlet oxygen sensitized photooxygenation of a bio-based molecule. The process allowed accurate control of irradiation (LED-driven spiral-shaped microreactor), light absorption (tunable absorbance) and flow conditions (slurry Taylor flow). The efficiency of the swollen RB-grafted colloids in converting α-terpinene into ascaridole with high conversion and high selectivity in short residence times has been clearly demonstrated. The efficiency was combined with sustainability of the process involving a green solvent (ethanol) and air as a less hazardous source of oxygen. The supported RB exhibited a reactivity similar to that of the free RB. Moreover, the photo-reactivity of RB-supported microgels was stable over 8 months of storage with good reproducibility. The photoactive colloids also proved to be reusable during several cycles. Finally, with a stoichiometric excess of α-terpinene compared to oxygen, in presence of high photon flux and for the highest concentration of Rose Bengal photosensitizer, the VBRB@MG colloids allowed the RB photobleaching levels to be decreased compared to free RB. This important result suggests that the covalent anchoring of RB molecules inside submicronic polymer colloids can prevent their photodegradation.

ASSOCIATED CONTENT

The Supporting Information includes Chemicals (section S.1), Main colloidal features of microgels (section S.2), UV-VIS absorption spectra (section S.3), LED array: emission spectrum and radiant power (section S.4), Gas-liquid Taylor flows (section S.5), Monitoring of the operating parameters and relationships between them (Section S.6), Absorbance of the reaction

medium and Photobleaching level (section S.7), Conversion of α-terpinene and yield of ascaridole (section S.8), Conditioning of the photoactive colloids synthesized for their implementation under reactive conditions (section S.9), Additional data related to Figures 2, 3 and 4 (section S.10), and Experiments to test the reusability of the photoactive colloids (section S.11).

Author Contributions

The manuscript was written through contributions of all authors. All authors have approved the final version of the manuscript.

Funding Sources

This work was sponsored by the French National Research Agency (ANR) under the Collaborative Research Project Program PICPOSS (ANR-15-CE07-0008-01).

Notes

The authors declare no competing financial interest.

ACKNOWLEDGMENT

The authors thank the French Research Agency for the funding under its Collaborative Research Project PICPOSS (ANR-15-CE07-0008-01). The authors also thank Jean-Claude Moschetti from CNRS for the picture illustrating the LED-driven spiral-shaped microreactor.

ABBREVIATIONS

A, absorbance; DLS, Dynamic Light Scattering; DVA, divinyl adipate; EtOH, ethanol; FEP, Fluorinated Ethylene Propylene tube; GC, gas chromatography; LED, Light-Emitting Diode;

MG, Microgel colloid; PSS, photosensitizers supported; RB, Rose Bengal; SR, Swelling ratio; TEM, Transmission Electron Microscopy); VAc, vinyl acetate; VCL, N-vinyl caprolactam; VBRB, vinyl benzyl Rose Bengal; αT, α-terpinene.

REFERENCES

1 Ciana, C.-L.; Bochet, C. G. Clean and Easy Photochemistry. *Chimia* **2007**, 61, 650. DOI: 10.2533/chimia.2007.650-654.

2 Hoffmann, N. Photochemical Reactions as Key Steps in Organic Synthesis. *Chem. Rev.* **2008**, 108, 1052-1103. DOI:10.1021/cr0680336.

3 Bach, T.; Hehn, J. P. Photochemical Reactions as Key Steps in Natural Product Synthesis. *Angewandte Chemie, International Edition* **2011**, 50, 5, 1000-1045. DOI:10.1002/anie.201002845.

4 Turro, N. J. Geometric and Topological Thinking in Organic Chemistry. *Angewandte Chemie, International Edition* **1986**, 25, 882-901. DOI:10.1002/anie.198608821.

5 Olivucci, M.; Santoro F. Chemical Selectivity Through Control of Excited- State Dynamics. *Angewandte Chemie, International Edition* **2008**, 47, 6322-6325. DOI:10.1002/anie.200800898.

6 Schapiro, I.; Melaccio, F.; Laricheva, E. N.; Olivucci, M. Using the Computer to Understand the Chemistry of Conical Intersections. *Photochem. Photobiol. Sci.* **2011**, 10, 867-886. DOI: 10.1039/c0pp00290a.

7 Hoffmann, N. Photochemical Reactions of Aromatic Compounds and the Concept of the Photon as a Traceless Reagent. *Photochem. Photobiol. Sci*. **2012**, 11, 1613-1641. DOI:10.1039/C2PP25074H.

8 Anastas, P. T.; Warner, J. C. Green Chemistry: Theory and Practice; Oxford University Press: New York, **1998**.

9 DeRosa, M.C.; Crutchley, R.J. Photosensitized Singlet Oxygen and its Applications. *Coord. Chem. Rev*. **2002**, 233, 351-371. DOI: 10.1016/S0010-8545(02)00034-6.

10 Ghogare, A. A.; Greer, A. Using Singlet Oxygen to Synthesize Natural Products and Drugs. *Chem. Rev*., **2016**. 116, 9994-10034. DOI:10.1021/acs.chemrev.5b00726.

11 Clennan, E. L.; Pace, A. Advances in Singlet Oxygen Chemistry. *Tetrahedron* **2005**, 61, 28, 6665-6691. DOI: 10.1016/j.tet.2005.04.017.

12 Alberti, M.N.; Vassilikogiannakis, G.; Orfanopoulos, M. Stereochemistry of Singlet Oxygen Simple Alkenes: A Stereospecific Transformation. *Org. Lett.* **2008**, 10, 3997-4000. DOI: 10.1021/ol801488w.

13 Iesce, M. R.; Cermola, F. Photooxygenation, [2+2] and [4+2]. In Organic Photochemistry and Photobiology, 3rd ed., Vol. 1 (Eds.: A. Griesbeck, M. Oelgemöller, F. Ghetti), CRC Press, Boca Raton, **2012**, 727-765.

14 Camussi, I.; Mannucci, B.; Speltini, A.; Profumo, A.; Milanese, C.; Malavasi, L; Quadrelli, P. g-C_3N_4 - Singlet Oxygen Made Easy for Organic Synthesis: Scope and Limitations. *ACS Sustainable Chem. Eng.* **2019**, 7, 9, 8176-8182. DOI: 10.1021/acssuschemeng.8b06164.

15 Díez-Mato, E.; Cortezón-Tamarit, F.C.; Bogialli, S.; García-Fresnadillo, D.; Marazuela M.D. Phototransformation of Model Micropollutants in Water Samples by Photocatalytic Singlet Oxygen Production in Heterogeneous Medium. *Appl. Catal., B* **2014** 160–161, 445-455. DOI:10.1016/j.apcatb.2014.05.050.

16 Manjon, F.; Villen, L.; Garcia-Fresnadillo D.; Orellana, G. On the Factors Influencing the Performance of Solar Reactors for Water Disinfection with Photosensitized Singlet Oxygen. *Environ. Sci. Technol.* **2008**, 42, 1, 301-307. DOI:10.1021/es071762y.

17 Magaraggia, M.; Faccenda, F.; Gandolfi A.; Jori, G. Treatment of Microbiologically Polluted Aquaculture Waters by a Novel Photochemical Technique of Potentially Low Environmental Impact. *J. Environ. Monit.* **2006**, 8, 9, 923-931. DOI: 10.1039/b606975d.

18 Gollnick, K. Photooxygenation and its Application in Industry. *Chim. Ind.* **1982**, 63, 156-166.

19 Braun, A.M.; Peschl, G.; Oliveros, E. Industrial Photochemistry. Handbook of Organic Photochemistry and Photobiology 3rd ed. CRC Press **2014**.

20 Paddon, C. J.; Westfall, P.; Pitera, D.; Benjamin, K.; Fisher, K.; et al. High-Level Semi-Synthetic Production of the Potent Antimalarial Artemisinin. *Nature* **2013**, 496, 528-532. DOI:10.1038/nature12051.

21 Turconi, J.; Griolet, F.; Guevel, R.; Oddon, G.; Villa, R.; Geatti, A.; Hvala, M.; Rossen, K.; Göller, R.; Burgard, A. Semisynthetic Artemisinin, the Chemical Path to Industrial Production. *Org. Process Res. Dev.* **2014**, *18*, 417-422. DOI:10.1021/op4003196.

22 Wootton, R. C. R.; Fortt, R.; De Mello, A. J. A Microfabricated Nanoreactor for Safe, Continuous Generation and Use of Use of Singlet Oxygen. *Org. Process Res. Dev*. **2002**, 6, 2, 2000–2002. DOI:10.1021/op0155155.

23 Coyle, E.E.; Oelgemöller, M. Micro-Photochemistry: Photochemistry in Microstructured Reactors. The new photochemistry of the future? *Photochem. Photobiol. Sci*. **2008**, 7, 1313-1322. DOI:10.1039/B808778D.

24 Oelgemöller, M. Highlights of Photochemical Reactions in Microflow Reactors. *Chem. Eng. Technol.* **2012**, 35, 7, 1144–1152. DOI:10.1002/ceat.201200009.

25 Cambié, D.; Bottecchia, C.; Straathof, N. J. W.; Hessel, V.; Noël, T. Applications of Continuous-Flow Photochemistry in Organic Synthesis, Material Science, and Water Treatment. *Chem. Rev*. **2016**, 116, 17, 10276-1034. DOI:10.1021/acs.chemrev.5b00707.

26 Mizuno, K.; Nishiyama, Y.; Ogaki, T.; Terao, K.; Ikeda, H.; Kakiuchi, K. Utilization of Microflow Reactors to Carry out Synthetically Useful Organic Photochemical Reactions.

J. Photochem. Photobiol., C Rev. **2016**, 29, 107–147. DOI 10.1016/j.jphotochemrev.2016.10.002.

27 Zhao, F.; Cambié, D.; Janse, J.; Wieland, E.W.; Kuijpers, K.P.L; Hessel, V.; Debije, M.G.; Noël, T. Scale-up of a Luminescent Solar Concentrator-Based Photomicroreactor via Numbering-up. *ACS Sustainable Chem. Eng.* **2018**, 6, 1, 422-429. DOI: 10.1021/acssuschemeng.7b02687.

28 Loubière, K.; Oelgemöller, M.; Aillet, T.; Dechy-Cabaret, O.; Prat, L. Continuous-Flow Photochemistry: A Need for Chemical Engineering. *Chem. Eng. Process.* **2016**, 104, 120-132. DOI:10.1016/j.cep.2016.02.008.

29 Haas, C.P.; Roider, T.; Hoffmann, R.W.; Tallarek, U. Light as a Reaction Parameter – Systematic Wavelength Screening in Photochemical Synthesis. *React. Chem. Eng.* **2019**, 4, 1912-1916. DOI: 10.1039/c9re00339h

30 Sender, M. ; Ziegenbalg, D. Light Sources for Photochemical Processes – Estimation of Technological Potentials. *Chem. Ing. Tech.* **2017**, 89, 1159–1173. DOI: 10.1002/cite.201600191 .

31 Loponov, K. N.; Lopes, J.; Barlog, M.; Astrova, E. V.; Malkov, A. V.; Lapkin, A. A. Optimization of a Scalable Photochemical Reactor for Reactions with Singlet Oxygen, *Org. Process Res. Dev*. **2014** 18, 11, 1443–1454.

32 Park, C. P. Y.; Kim, Y. J.; Lim, H. J.; Park, J. H.; Kim, M. J.; Seo, S. W.; Park, C. P. Continuous Flow Photooxygenation of Monoterpenes *RSC Adv.* **2015**, 5, 6, 4233–4237. DOI:10.1039/C4RA12965B.

33 Radjagobalou, R.; Blanco, J-F.; Dechy-Cabaret, O.; Oelgemöller, M., Loubière, K. Photooxygenation in an Advanced Led-Driven Flow Reactor Module: Experimental

Investigations and Modelling. *Chem. Eng. Process* **2018**, 130, 214-228. DOI: 10.1016/j.cep.2018.05.015.

34 Horn, C; Gremetz, S. A method to determine the correct photocatalyst concentration for photooxidation reactions conducted in continuous flow reactors. *Beilstein J. Org. Chem.* **2020**, 16, 871–879. DOI:10.3762/bjoc.16.78 .

35 Chaudhuri, A.; Kuijpers, K. P. L.; Hendrix, R. B. J.; Shivaprasad, P.; Hacking, J.A.; Emanuelsson, E.A.C.; Noël, T.; van der Schaaf, J. Process intensification of a photochemical oxidation reaction using a Rotor-Stator Spinning Disk Reactor: A strategy for scale up. *Chem. Eng. J.* **2020**, 400, 125875. DOI: 10.1016/j.cej.2020.125875 .

36 Lee, D. S.; Sharabi, M.; Jefferson-Loveday, R.; Pickering, S. J.; Poliakoff, M.; George, M. W. Scalable Continuous Vortex Reactor for Gram to Kilo Scale for UV and Visible Photochemistry. *Org. Process Res. Dev*. **2020**, 24, 201–206. DOI: 10.1021/acs.oprd.9b00475.

37 Lacombe, S.; Soumillion, J.-P.; Pigot, T.; Blanc, S.; Brown, R.; Oliveros, E.; Cantau, C.; Saint-Cricq, P. Solvent-Free Production of Singlet Oxygen at the Gas-Solid Interface: Visible Light Activated Organic-Inorganic Hybrid Microreactors Including New Cyanoaromatic Photosensitizers. *Langmuir* **2009**, 25, 1 1168-11179. DOI: 10.1021/la901504q.

38 Ronzani, F.; Costarramone, N.; Blanc, S.; Le Bechec, M.; Pigot, T.; Oelgemöller, M.; Lacombe. S. Visible-Light Photosensitized Oxidation of Alpha-Terpinene using Novel Silica-Supported Sensitizers: Photooxygenation vs. Photodehydrogenation. *J. Catal.* **2013**, 303, 164-174. DOI: 10.1016/j.jcat.2013.04.001.

39 Lapkin, A.A.; Boddub, V.M.; Aliev G.A.; Goller, B.; Polissk, S.; Kovalev, D. Photo-Oxidation by Singlet Oxygen Generated on Nanoporous Silicon in a LED-Powered Reactor. *Chem. Eng. J*., **2008**, 136, 331–336. DOI:10.1016/j.cej.2007.04.013.

40 Lacombe, S; Pigot, T. Materials for Selective Photo-oxygenation vs. Photocatalysis: Preparation, Properties and Applications in Environmental and Health Fields. *Catal. Sci. Technol*. **2016**, 6, 1571-1592. DOI: 10.1039/C5CY01929J.

41 Mosinger, J., Lang, K.; Plistil, L.; Jesenska, S.; Hostomsky, J.; Zelinger; Z. Fluorescent Polyurethane Nanofabrics: A Source of Singlet Oxygen and Oxygen Sensing *Langmuir* **2010**, 26, 10050-10056. DOI:10.1021/la1001607.

42 Zhang, Y.; Wang, W.; Li. Efficient Photooxygenation of Furans using Oxygen with Wool-Immobilizing Rose Bengal as Green Photosensitizer. *Asian J. Chem*., **2015**, 27, 1, 111-116. DOI:10.14233/ajchem.2015.16745

43 Ronzani, F; Saint-Cricq, P; Arzoumanian, E; Pigot, T; Blanc, S; Oelgemöller, M; Oliveros, E; Richard, C; Lacombe, S. Immobilized Organic Photosensitizers with Versatile Reactivity for various Visible-Light Applications. *Photochem Photobiol*., **2014**, 90, 2, 358-368. DOI: 10.1111/php.12166.

44 Dambruoso, P.; Ballestri, M.; Ferroni, C.; Guerrini, A.; Sotgiu, G.; Varchi, G.; Massi, A. TPPS Supported on Core–Shell PMMA Nanoparticles: the Development of Continuous-Flow Membrane-Mediated Electrocoagulation as a Photocatalyst Processing Method in Aqueous Media. *Green Chem*. **2015,** 17, 1907-1917. DOI:10.1039/C4GC01996B

45 Shen, J.; Steinbach, R.; Tobin, J. M.; Nakata, M. M.; Bower, M.; McCoustra, M. R. S.; Bridle, H.; Arrighi, V.; Vilela, F. Photoactive and metal-free polyamide-based polymers

for water and wastewater treatment under visible light irradiation . *Appl. Cat. B: Environ*. **2016**, 193, 1873-3883. DOI: 10.1016/j.apcatb.2016.04.015

46 Valverde, D.; Porcar, R.; Izquierdo, D.; Burguete, M. I.; Garcia-Verdugo, E.; Luis, S. V. Rose Bengal Immobilized on Supported Ionic-Liquid-like Phases: An Efficient Photocatalyst for Batch and Flow Processes. *ChemSusChem* **2019**, 12, 17, 3996-4004. DOI: 10.1002/cssc.201901533.

47 Carofiglio, T.; Donnola, P.; Maggini, M.; Rossetto, M.; Rossi, E. Fullerene-Promoted Singlet-Oxygen Photochemical Oxygenations in Glass-Polymer Microstructured Reactors. *Adv Synth Catal* **2008**, 350, 2815-2822. DOI: 10.1002/adsc.200800459.

48 Han, X., Bourne, R.A.; Poliakoff, M.; George, M.W. Immobilised Photosensitisers for Continuous Flow Reactions of Singlet Oxygen in Supercritical Carbon Dioxide. *Chem. Sci*. **2011**, 2, 1059-1067. DOI:10.1039/C0SC00641F.

49 Lumley, E. K.; Dyer, C. E.; Pamme, N.; Boyle, R. W. Comparison of Photo-Oxidation Reactions in Batch and a New Photosensitizer-Immobilized Microfluidic Device. *Org. Lett*. **2012**, 14, 22, 5724–5727. DOI:10.1021/ol3023424.

50 Amara, Z.; Bellamy, J.F.B; Horvath, R.; Miller, S.J.; Beeby, A.; Burgard, A.; Rossen, K.; Poliakoff, M.; George, M.W. Applying Green Chemistry to the Photochemical Route to Artemisinin. *Nature Chemistry* **2015**, 7, 489-495. DOI: 10.1038/NCHEM.2261.

51 Tobin, J.M.; McCabe, T. J.D.; Prentice A.W.; Holzer, S.; Lloyd, G.O., Paterson, M.J., Arrighi, V., Cormack, P.A.G.; Vilela, F. Polymer-Supported Photosensitizers for Oxidative Organic Transformations in Flow and under Visible Light Irradiation. *ACS Catal.* **2017**, 7, 4602−4612. DOI: 10.1021/acscatal.7b00888.

52 Kong, C.J.; Fisher, D.; Desai, B.K.; Yang, Y.; Ahmad, S.; Belecki, K.; Gupton, B.K. High Throughput Photo-Oxidations in a Packed Bed Reactor System. *Bioorg Med Chem.* **2017**, 25, 23, 6203-6208. DOI:10.1016/j.bmc.2017.07.004.

53 Masuda, K.; Wang, Y.; Onozawa, S-Y.; Shimada, Y.; Koumura, N.; Sato, K.; Kobayashi, S. Robust Organic Photosensitizers Immobilized on a Vinylimidazolium Functionalized Support for Singlet Oxygen Generation under Continuous-Flow Conditions. *Synlett* **2020**, 31, 497–501. DOI: 10.1055/s-0039-1691582.

54 Blanchard, F.; Asbai, Z.; Cottet, K ; Boissonnat, G.; Port, M.; Amara, Z. Continuous Flow Photo-Oxidations Using Supported Photocatalysts on Silica. *Org. Process Res. Dev*. **2020**, 24, 5, 822-826. DOI :10.1021/acs.oprd.9b00420

55 Thomson, C.G.; Jones, C.M. S.; Rosair, G.; Ellis, D. ; Marques-Hueso, J.; Lee, A-L; Vilela, F. Continuous-Flow Synthesis and Application of Polymer-Supported BODIPY Photosensitisers for the Generation of Singlet Oxygen; Process Optimised by In-Line NMR Spectroscopy. *J. Flow Chem.* **2020**, 10, 327–345. DOI:10.1007/s41981-019-00067-4

56 Tobin, J. M.; Liu, J.; Hayes, H.; Demleitner, M.; Ellis, D.; Arrighi, V.; Xu, Z.; Vilela, F. BODIPY-Based Conjugated Microporous Polymers as Reusable Heterogeneous Photosensitisers in a Photochemical Flow Reactor. *Polym. Chem*. **2016**, 7, 6662-6670.DOI: 10.1039/c6py01393g.

57 Enache, D.I.; Hutchings, G.J.; Taylor, S.H.; Stitt, E.H. The Hydrogenation of Isophorone to Trimethyl Cyclohexanone Using the Downflow Single Capillary Reactor. *Cat. Today* **2005**, 105, 569-573. DOI:10.1016/j.cattod.2005.06.013.

58 Enache, D.I.; Hutchings, G.J.; Taylor, S.H.; Raymahasay, S.; Winterbottom, J.M.; Raymahasay, S.; Mantle, M.D.; Sederman A.D.; Gladden, L.F.; Chatwin, C.; Symonds, K.T.; Stitt, H. Multiphase Hydrogenation of Resorcinol in Structured and Heat Exchange Reactor Systems: Influence of the Catalyst and the Reactor Configuration. *Cat. Today* **2007**, 128, 26-35. DOI: 10.1016/j.cattod.2007.08.012.

59 Buisson, B.; Donegan, S.; Wray, D.; Parracho, A.; Gamble, J.; Caze, P.; Jorda, J.; Guermeur, C. Slurry Hydrogenation in a Continuous Flow Reactor for Pharmaceutical Application. *Chem. Today* **2009**, 27, 12-15.

60 Mendoza, C.; Emmanuel, N.; Páez, C.A.; Dreesen, L.; Monbaliu, J-C; Heinrichs, B. Improving Continuous Flow Singlet Oxygen Photooxygenations with Functionalized Mesoporous Silica Nanoparticles. *ChemPhotoChem*. **2018**, 2, 10, 890-897. DOI:10.1002/cptc.201800148.

61 Ogilby, PR. Singlet Oxygen: There is still something new under the Sun, and Ii is better than ever. *Photochem. Photobiol. Sci*. **2010**, 9, 1543-1560. DOI:10.1039/C0PP00213E.

62 Schweitzer, C; Schmidt, R. Physical Mechanisms of Generation and Deactivation of Singlet Oxygen. *Chem. Rev.*, **2003**, 103, 1685–1758. DOI:10.1021/cr010371d

63 Petrizza, L.; Le Bechec, M.; Decompte, E.; El Hadri, H.; Lacombe, S.; Save, M. Tuning Photosensitized Singlet Oxygen Production from Colloids Synthesized by Polymerization in Aqueous Dispersed Media, *Polym. Chem*. **2019**, 10, 23, 3170–3179. DOI:10.1039/C9PY00157C.

64 Wilkinson, F.; Helman, W.P.; Ross, A.B. Quantum Yields for the Photosensitized Formation of the Lowest Electronically Excited Singlet State of Molecular Oxygen in Solution. *J. Phys. Chem. Ref. Data* **1993**, 22, 113-262. DOI:10.1063/1.555934.

65 Wilkinson, F.; Helman, W. P.; Ross, A. B. Rate Constants for the Decay and Reactions of the Lowest Electronically Excited Singlet State of Molecular Oxygen in Solution. An Expanded and Revised Compilation. *J. Phys. Chem. Ref. Data* **1995**, 24, 2, 663-1021. DOI:10.1063/1.555965.

66 Etchenausia, L.; Malho Rodrigues, A.; Harrisson, S.; Deniau-Lejeune, E.; Save, M. "RAFT Copolymerization of Vinyl Acetate and N-Vinylcaprolactam: Kinetics, Control, Copolymer Composition and Thermoresponsive Self-Assembly. *Macromolecules* **2016**, 49, 18, 6799–6809. DOI: 10.1021/acs.macromol.6b01451

67 Aillet, T.; Loubière, K., Dechy-Cabaret, O., Prat, L. Microreactors as a Tool for Acquiring Kinetic Data on Photochemical Reactions. *Chem. Eng. Technol.* **2016**, 39, 1, 115-122.

68 Mei, M.; Felis, F.; Dietrich, N.; Hébrard, G.; Loubière, K. Hydrodynamics of Gas-Liquid Slug Flows in a Long In-Plane Spiral-Shaped Milli-Reactor *Theor. Found. Chem. Eng.* **2020**, 54, 1, 25-47. DOI: 10.1134/S0040579520010169.

69 Mei, M.; Dietrich, N.; Hébrard, G.; Loubière, K. Gas-Liquid Mass Transfer around Taylor Bubbles Flowing in a Long In-Plane Spiral-Shaped Milli-Reactor. *Chem. Eng. Sci*. **2020**, 222, 115717. DOI:10.1016/j.ces.2020.115717

70 Liedtke, A.K.; Bornette, F.; Philippe, R.; de Bellefon, C. Gas–Liquid–Solid ''Slurry Taylor'' Flow: Experimental Evaluation through the Catalytic Hydrogenation of 3-methyl-1-pentyn-3-ol. *Chem. Eng. J*. **2013**, 227, 174-181. DOI:10.1016/j.cej.2012.07.100.

71 Liedtke, A.K.; Bornette, F.; Philippe, R.; de Bellefon, C. External Liquid Solid Mass Transfer for Solid Particles Transported in a Milli-Channel Within a Gas-Liquid Segmented Flow. *Chem. Eng. J*. **2015**, 287, 92-102. DOI:10.1016/j.cej.2015.10.109

72 Krasnovsky, A. A. Jr.; Roumbal, Y. V.; Strizhakov, A. A. Rates of $^{1}O2$ ($^{1}\Delta g$) Production upon Direct Excitation of Molecular Oxygen by 1270 nm Laser Radiation in Air-Saturated Alcohols and Micellar Aqueous Dispersions. *Chem. Phys. Lett*. **2008**, 458, 195–199. DOI:10.1016/j.cplett.2008.04.091.

73 Zakrzewski, A.; Neckers, D.C. Bleaching Products of Rose Bengal under Reducing Conditions. *Tetrahedron* **1987**, 43, 20, 4507-4512.

74 Neckers, D.C. Rose Bengal. *J. Photochem. Photobio. A Chem.* **1989**, 47, 1-29. DOI:10.1016/1010-6030(89)85002-6.

75 Binks, B.P. Particles as Surfactants—Similarities and Differences. *Curr. Opin. Colloid Interface Sci.* **2020**, 7, 21-41. DOI:10.1016/S1359-0294(02)00008-0.

76 Valadbaigi, P.; Ettelaie, R.; Kulak, A.N.; Murray, B.S. Generation of Ultra-Stable Pickering Microbubbles via Poly Alkylcyanoacrylates. *J. Colloid Interface Sci.* **2019**, 536, 618-627. DOI:10.1016/j.jcis.2018.10.004.

77 Li, X.; Murray, B.S.; Yang, Y.; Sarkar, A. Egg White Protein Microgels as Aqueous Pickering Foam Stabilizers: Bubble Stability and Interfacial Properties. *Food Hydrocolloids* **2020**, 98, 105-292. DOI:10.1016/j.foodhyd.2019.105292.

TOC/ABSTRACT GRAPHICS

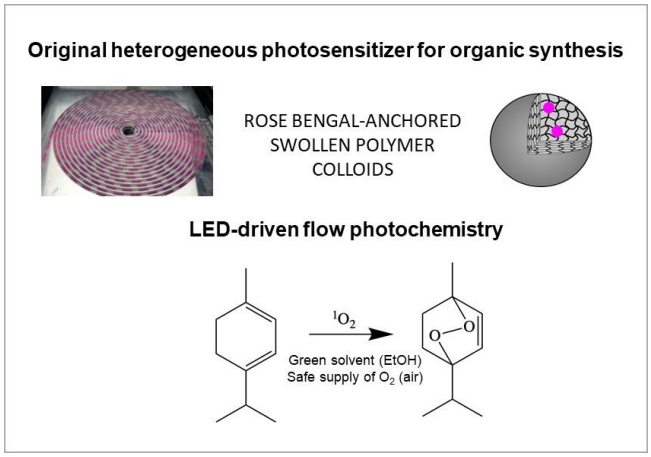

SYNOPSIS

Combining polymer swollen colloids and flow photochemistry for sustainable singlet oxygen sensitized photooxygenation of a bio-based molecule